Spatiotemporal fractionation schemes for liver stereotactic body radiotherapy

Unkelbach, Jan ; Papp, Dávid ; Gaddy, Melissa R ; Andratschke, Nicolaus ; Hong, Theodore ; Guckenberger, Matthias

DOI: https://doi.org/10.1016/j.radonc.2017.09.003

Originally published at:
Unkelbach, Jan; Papp, Dávid; Gaddy, Melissa R; Andratschke, Nicolaus; Hong, Theodore; Guckenberger, Matthias (2017). Spatiotemporal fractionation schemes for liver stereotactic body radiotherapy. Radiotherapy and Oncology, 125(2):357-364.
DOI: https://doi.org/10.1016/j.radonc.2017.09.003

Spatiotemporal fractionation schemes for liver stereotactic body radiotherapy

Short title: **Spatiotemporal fractionation for liver SBRT**

First author and corresponding author:

Jan Unkelbach, PhD
Department of Radiation Oncology
University Hospital Zürich
Mail: Rämistrasse 100, 8091 Zürich, Switzerland
Email: jan.unkelbach@usz.ch
Phone: +41 44 255 3742

Coauthors:

Dávid Papp, PhD
Department of Mathematics, North Carolina State University, Rayleigh, NC, USA

Melissa R. Gaddy
Department of Mathematics, North Carolina State University, Rayleigh, NC, USA

Nicolaus Andratschke, MD
Department of Radiation Oncology, University Hospital Zürich, Switzerland

Theodore Hong, MD
Department of Radiation Oncology, Massachusetts General Hospital, Boston, MA, USA

Matthias Guckenberger, MD
Department of Radiation Oncology, University Hospital Zürich, Switzerland

Keywords:
liver SBRT; dose escalation; fractionation; treatment plan optimization

Conflicts of interest:
None

Acknowledgements:
The project was in parts supported by the National Cancer Institute (grant U19 CA021239-35) and the Federal Share of program income earned by Massachusetts General Hospital on C06 CA059267, Proton Therapy Research and Treatment Center. In addition, this this work was partially supported by the National Science Foundation under Grant DMS-1127914 to the Statistical and Applied Mathematical Sciences Institute.

Abstract:

Background and Purpose: Dose prescription in stereotactic body radiotherapy (SBRT) for liver tumors is often limited by the mean liver dose. We explore the concept of spatiotemporal fractionation as an approach to facilitate further dose escalation in liver SBRT.

Materials and Methods: Spatiotemporal fractionation schemes aim at partial hypofractionation in the tumor along with near-uniform fractionation in normal tissues. This is achieved by delivering distinct dose distributions in different fractions, which are designed such that each fraction delivers a high single fraction dose to complementary parts of the tumor while creating a similar dose bath in the surrounding noninvolved liver. Thereby, higher biologically effective doses (BED) can be delivered to the tumor without increasing the mean BED in the liver. Planning of such treatments is performed by simultaneously optimizing multiple dose distributions based on their cumulative BED. We study this concept for five liver cancer patients with different tumor geometries.

Results: Spatiotemporal fractionation presents a method of increasing the ratio of prescribed tumor BED to mean BED in the noninvolved liver by approximately 10-20%, compared to conventional SBRT using identical fractions.

Conclusions: Spatiotemporal fractionation may reduce the risk of liver toxicity or facilitate dose escalation in liver SBRT in circumstances where the mean dose to the non-involved liver is the prescription-limiting factor.

Introduction:

Clinical motivation:
Liver stereotactic body radiotherapy (SBRT) has become an established treatment option for primary and metastatic liver cancer [1-9]. For large tumors, the prescription dose is often limited by the mean dose delivered to the noninvolved liver. This reduces the chance of loco-regional tumor control and warrants the exploration of novel concepts to allow for further dose escalation [4, 8].

Spatiotemporal fractionation:
Fractionated treatments face a tradeoff. Increasing the number of fractions is desirable to protect normal tissues. However, the total dose must be increased to maintain tumor control [10]. In that sense, the ideal treatment would simultaneously facilitate hypofractionation in tumors along with near-uniform fractionation in normal tissues. Recently, it has been shown that this goal can be achieved to some degree by delivering distinct dose distributions in different fractions. The concept has been named spatiotemporal fractionation [11-14].

The concept was initially demonstrated for proton therapy [13, 14] and subsequently for conventional photon beams [11, 12]. The rationale can be understood in the context of

rotation therapy delivered with tomotherapy or volumetric-modulated arc therapy (VMAT). Distinct VMAT plans for different fractions can be designed in such a way that each fraction delivers a similar dose bath to the normal tissue surrounding the tumor (i.e. exploits the fractionation effect). However, each fraction delivers a high single-fraction dose to different parts of the target volume. Thereby, some degree of hypofractionation is achieved in the tumor along with near-uniform fractionation in normal tissues. Spatiotemporal fractionation was outlined as an approach to improve fractionated radiosurgery for large cerebral arteriovenous malformations [12].

In this report, we investigate the potential of spatiotemporal fractionation to improve the ratio of tumor BED to mean liver BED in liver SBRT. Thereby, the approach may reduce the risk of radiation-induced side effects in the liver. Alternatively, spatiotemporal fractionation may facilitate dose escalation in liver SBRT in circumstances where the mean dose to the non-involved liver is the prescription-limiting factor.

Methods

Patients:
We demonstrate spatiotemporal fractionation for 5 liver cancer patients shown in Figure 1. These patients were selected as to represent a spectrum of tumor geometries, locations and sizes. Patient 1 has 4 metastases of varying size located throughout the right lobe of the liver and is discussed in detail in the results section. The total GTV volume is 391 cc and the mean liver dose is the dose-limiting constraint. Characteristics of patients 2-5 are described in the supplementary materials, Appendix A.

Modeling of fractionation effects:
We consider SBRT treatments with 5 fractions and assume that the fractionation schemes summarized in Table 1 are isoeffective. These fractionation effects can be modeled via the BED model [10, 15] using generic values for the α/β-ratio, i.e. $\alpha/\beta = 10$ in the tumor and $\alpha/\beta = 4$ in all normal tissues. For example, 50 Gy delivered to the tumor in 5 fractions is equivalent to 27 Gy in a single fraction, and both regimens correspond to a BED_{10} of 100 Gy.

For spatiotemporal fractionation, we assume that the BED model can be extended to non-stationary fractionation schemes, in which the dose varies from fraction to fraction. In voxel *i*, the cumulative BED b_i of all fractions is given by

$$b_i = \sum_{t=1}^{n} \left(d_{it} + \frac{d_{it}^2}{(\alpha/\beta)_i} \right)$$

where d_{it} is the dose delivered in fraction *t*, *n* is the number of fractions, and $(\alpha/\beta)_i$ is the α/β-ratio of the structure that voxel *i* belongs to.

For visualization and quantitative interpretation, the BED can be scaled by a factor $1/[1 + X/(\alpha/\beta)]$, where *X* is a reference dose level [16]. In this report, we set *X* to 8 Gy, i.e. to the prescribed dose per fraction in the PTV. This yields the equieffective dose

$$EQD8 = \frac{b}{\left[1 + \frac{8}{(\alpha/\beta)}\right]}$$

$EQD8$ can be interpreted as the total physical dose that needs to be delivered in a uniformly fractionated treatment with a dose of 8 Gy per fraction to achieve the BED *b*.

Treatment plan optimization:
We simultaneously optimize multiple IMRT plans based on their cumulative BED distribution. Traditional treatment plan optimization for IMRT is performed using objective and constraint functions evaluated for physical dose. Here, we apply the same functions with the difference that these are evaluated for cumulative BED rather than physical dose. To derive BED constraints for normal tissues and BED prescriptions for the target volume, typical constraints and prescriptions for 5-fraction liver SBRT were converted into BED[1]. We consider the following treatment planning problem:

Constraints:

1. The maximum BED_4 to the bowel, duodenum and stomach is constrained to 75 Gy, corresponding to 30 Gy physical dose in 5 fractions.

Objectives:

1. A BED_{10} of 100 Gy is prescribed to the GTV (implemented via quadratic penalty functions). This corresponds to 50 Gy physical dose delivered in 5 fractions.
2. A BED_{10} of 72 Gy is prescribed to the PTV, corresponding to 40 Gy physical dose in 5 fractions. A BED_{10} exceeding 100 Gy is penalized quadratically.
3. A BED_4 to the chest wall exceeding 120 Gy, corresponding to 40 Gy physical dose in 5 fractions, is penalized quadratically.
4. The plan is to be conformal (implemented via quadratic penalty functions where the allowed dose decreases linearly with distance from the PTV). A dose falloff to half the PTV prescription dose at 1 cm distance from the PTV is aimed for.
5. The mean BED_4 to the healthy tissue excluding the PTV and the liver is minimized.
6. The mean BED_4 to the liver excluding the GTV is minimized.

We first optimize a treatment plan that delivers the same dose in each fraction, which we call the *reference plan*. This is done based on a weighted sum of the 6 objectives. Second, we optimize two spatiotemporal plans:

1. Spatiotemporal plan 1 is obtained for optimizing the same objective function as for the reference plan, i.e. the same relative weighting of the 6 objectives. Hence, the benefit of spatiotemporal fractionation is distributed over all objectives.

[1] Prescription doses and normal tissue constraints are based on a Phase III trial to evaluate the efficacy of proton therapy against photon therapy conducted at Massachusetts General Hospital (www.clinicaltrials.gov; Study title: Radiation Therapy with Protons or Photons in Treating Patients with Liver Cancer). These parameters also reflect institutional practice at University Hospital Zürich.

2. Spatiotemporal plan 2 is obtained by minimizing the mean liver BED, subject to the constraints that the plan is no worse that the reference plan for each of the other 5 objectives. Hence, the entire benefit of spatiotemporal fractionation is concentrated on reducing mean liver BED.

Details of treatment plan optimization are described in the supplementary materials, Appendix B. We consider IMRT plans consisting of 19 equispaced coplanar beams, which approximates the best coplanar rotation therapy plan, which could be delivered with tomotherapy or VMAT [17]. We use a beamlet resolution of 5x5 mm.

Results

Figure 2g shows the dose distribution for patient 1 for the reference plan that delivers the same dose distribution in all 5 fractions. The plan achieves a mean liver dose of 18.3 Gy, which is near or exceeding the tolerance for 5-fraction treatments [9, 18]. Hence, the mean liver dose represents the dose-limiting constraint. Figures 2a-e show the spatiotemporal treatment plan 2. Each fraction delivers a high single-fraction dose to complementary parts of the tumor. In some places, single fraction doses exceeding 25 Gy are delivered. Note that a single-fraction dose of 27 Gy delivers the prescribed BED_{10} of 100 Gy to the GTV. However, each fraction also delivers a similar dose bath to the surrounding healthy liver and thereby exploits the fractionation effect. Figure 2f illustrates the higher degree of fractionation in the liver compared to the target. It shows, voxel-by-voxel, the percentage of the total physical dose that is delivered by the fraction that contributes the highest dose. A value of 20% indicates perfectly uniform fractionation.

Figure 2k shows the equieffective dose EQD8 for the spatiotemporal treatment plan, demonstrating that all 5 fractions together deliver the prescribed BED to the target volume. Figure 2l shows the difference of EQD8 for the reference plan (Figure 2j) and the spatiotemporal plan (Figure 2k). Both treatments deliver approximately the same BED to the tumor, but the spatiotemporal plan yields lower mean BED in the noninvolved liver and the unclassified normal tissue. The mean liver BED is reduced by 12.8% when considering the liver without GTV, and by 17.3% when considering the liver without PTV (Table 2). This benefit originates from the fact that the spatiotemporal plan achieves the prescribed tumor BED with less physical dose. This can be seen in figures 2g-i, which show the cumulative physical dose in the reference plan, the spatiotemporal plan, and the difference. The mean physical dose in the GTV is reduced by 9.3%. Figure 3 compares reference and spatiotemporal plan in terms of the DVH evaluated for EQD8 (a) and dose (b).

Similar results have been obtained for other patients. The spatiotemporal treatment plans for patients 2-5 are shown in the supplementary materials, Appendix C1. Figure 4a shows the dose distributions of 2 out of 5 fractions for patient 5, who harbors a large tumor. The figure illustrates that dose distributions that achieve a high degree of fractionation in normal tissues along with hypofractionation in the tumor are not obvious and would be difficult to design manually. Through BED-based planning, all dose distributions are created automatically by the optimization algorithm without manually compartmentalizing the target volume a priori.

Summary of liver BED reductions

Table 2 summarizes the results in terms of mean liver BED reductions. Spatiotemporal 5-fraction treatments achieve a BED reduction of 10-20% in the noninvolved liver. As expected, the benefit is larger when considering liver without GTV as opposed to liver without PTV, because the degree to which near-uniform fractionation is achieved is better outside of the PTV than inside. Further discussion on Table 2 is provided in the supplementary materials, Appendix C2.

Critical structures abutting the PTV

For liver SBRT, the main OARs other than the liver are stomach, bowel, duodenum, and to a lesser degree the chest wall. For patient 4, the inferior part of the tumor is surrounded by chest wall, bowel and stomach. Assume the maximum BED_4 of 75 Gy is delivered to bowel and stomach. If this is done by delivering 6 Gy in each of the 5 fractions, the overlapping part of the PTV receives a BED_{10} of 48 Gy. If instead 15.4 Gy was delivered in a single fraction to reach the maximum BED_4 of 75 Gy, the BED_{10} to the PTV would drop to 39.1 Gy. The PTV underdose is hence minimized for uniform fractionation. In addition, the inferior part of the tumor is surrounded by almost no healthy liver tissue. Consequently, the benefit of spatiotemporal fractionation is small. This is illustrated in figure 4b, which shows that spatiotemporal planning for patient 4 results in a near-uniformly fractionated plan that avoids the high single-fraction doses observed for the other patient (see further discussion in the supplementary materials, Appendix C2).

Increasing the number of fractions

Above we considered 5-fraction SBRT treatments where each fraction delivers a distinct dose distribution. Spatiotemporal fractionation can also be applied to treatments with more fractions while delivering each dose distributions multiple times. For example, a 15-fraction treatment may consist of 5 distinct fractions that are delivered 3 times each. This may be desirable to increase the fractionation effect in normal tissues and to mitigate the impact of setup errors. Generally, it is expected that the benefit of spatiotemporal fractionation will decrease slightly if the number of fractions is increased (while keeping the number of distinct dose distributions equal to 5). This can be understood by considering the isoeffective fractionation schemes in Table 1. For 5-fractions treatments, the physical dose in the GTV can be reduced from 50 Gy to 27 Gy in places where the entire BED is delivered in a single fraction. This represents a 46% reduction in physical dose, which can in parts translate into normal tissue BED reduction depending on the degree of fractionation achieved there. For 15-fraction treatments (with 5 distinct fractions delivered 3 times each), the GTV dose can be reduced from 68.6 Gy (in 15 equal fractions) to 41.8 Gy (in places where the entire BED is delivered in 3 fractions). This corresponds to a 39% reduction in physical dose, i.e. slightly lower than for 5-fraction treatments. For 25-fraction treatments (with 5 distinct fractions delivered 5 times each), the physical dose can be lowered from 76.5 Gy to 50 Gy (35%). For the liver without PTV for patient 1, we observed a 11.1% mean liver BED reduction for 15-fraction treatments (5x3) and a 8.5% reduction for 25-fraction treatments (5x5), which agrees with the above considerations (Table 2).

Alternative spatiotemporal fractionation schemes

So far, we considered spatiotemporal treatments with 5 distinct fractions, leading to treatments where each fraction delivers high single fraction doses to complementary parts

of the target. Figure 4c shows an alternative 5-fraction scheme for patient 3 with only two distinct dose distributions. In this treatment, one plan is delivered 4 times and the second plan once. This leads to a treatment scheme in which the single fraction delivers a high dose to the center of the GTV, while the remaining 4 fractions primarily treat the PTV rim surrounding the GTV. This is an intuitive result: The single fraction hypofractionates the GTV while the remaining fractions achieve a high degree of fractionation in the normal liver adjacent to the GTV. However, the mean liver BED reduction compared to the reference plan was below 5% and hence small compared to treatment with 5 distinct fractions (Table 2).

Discussion

We demonstrate that spatiotemporal fractionation can reduce the mean liver BED by 10-20% for a fixed prescribed tumor BED. Thus, the approach may reduce the risk of radiation-induced side effects in the liver. Alternatively, spatiotemporal fractionation may facilitate dose escalation in liver SBRT in situations when the prescription dose is limited by the mean liver dose (rather than the bowel, stomach or duodenum). Depending on the location on the dose-response curve, this may translate into substantial improvements in tumor control probability [4]. Patients with large or multiple lesions that are mostly surrounded by functioning liver tissue are most likely to benefit from spatiotemporal fractionation. In contrast, patients in whom the prescription dose is limited due to the tumor's proximity to bowel, stomach or duodenum are less likely to benefit from spatiotemporal fractionation.

Stated vice versa, liver SBRT is a promising application for the concept of spatiotemporal fractionation as it fulfils the main requirements. First, the target volume mainly represents GTV that is eligible for hypofrationation rather than CTV where embedded normal tissue must be protected through fractionation. Second, spatiotemporal fractionation can primarily lower the mean dose to the surrounding normal tissues. In liver SBRT, the mean liver dose is often dose-limiting, rather than the maximum dose.

Quantifying the fractionation effect from clinical data is generally problematic and α/β-ratios are uncertain. This is in particular the case for liver toxicity endpoints because both fractionation effects and dose-volume effects need to be accounted for in outcome modeling. Generally, it is expected that the benefit of spatiotemporal fractionation over uniform fractionation decreases with lower α/β-ratio for the liver whereas a higher liver α/β-ratio is in favor of spatiotemporal fractionation [14]. However, the dependence of mean liver BED reductions on the α/β-ratio is weak within the range of typically assumed values, which was confirmed by treatment planning experiments. For example, for 5-fraction treatments, spatiotemporal plan 2 for patient 1 yields an improvement in mean BED in the liver excluding the PTV of 17.3% (Table 2). Changing the α/β-value in the liver mean BED objective to 2, 3, 4, 6, and 8 (while all other parameters remain unchanged) results in percentage mean BED reductions of 15.0, 16.3, 17.3, 18.7, and 19.5. This week dependence can also be understood based on the following consideration. In the healthy liver around the PTV, where the highest dose to normal tissue is expected, a uniformly fractionated SBRT plan delivers approximately a total physical dose of 40 Gy in 5 fractions. Assuming α/β = 4, this corresponds to a single-fraction dose of 20 Gy. If instead we assumed α/β = 3, this

would correspond to a single-fraction dose of 19.53 Gy. This indicates that changing the α/β-ratio for the normal tissue from 4 to 3 corresponds to a small change in what fractionation schemes are assumed to be isotoxic. Hence, changes of the α/β-ratio within the range of typically assumed values does not yield markedly different results regarding the properties of spatiotemporal treatment plans.

Respiratory motion and setup uncertainty is a concern regarding spatiotemporal fractionation for liver SBRT. In this work, it is assumed that the dose contributions of different fractions are delivered as planned and thereby add up to the prescribed BED in all parts of the target. Setup uncertainty may lead to misalignment of dose contributions of different fractions, potentially causing target underdosing. Future work should devise stochastic programming methods to incorporate uncertainty directly into treatment plan optimization. In conventional uniformly fractionated treatments, motion and setup uncertainty can be accounted for by margins. This approach has limitations in spatiotemporal fractionation. Here, the target volume is effectively compartmentalized into distinct regions that are treated in different fractions. The compartmentalization is not manually determined before treatment planning. It is optimized automatically during treatment plan optimization. Hence, it is not possible to manually design margins to account for inter-fraction setup errors. Therefore, stochastic programming or robust optimization methods [19-21] may be a necessity to handle setup uncertainty in planning. In addition, technologies currently under development may provide the tools to safely deliver spatiotemporal liver SBRT treatments in the future. This includes the development of MR-guided radiotherapy [22-24] as well as MLC and couch tracking [25-32].

Conclusions:

Spatiotemporal fractionation may improve the ratio of BED in the tumor to mean BED in the surrounding liver by approximately 10-20%. This is achieved by delivering distinct dose distributions in different fractions to facilitate partial hypofractionation in the tumor along with more uniform fractionation in the liver. Therefore, spatiotemporal fractionation may lower side effects or facilitate dose escalation in liver SBRT for patients in whom the prescription dose is limited by the mean liver dose.

Tables:

	total dose delivered in *n* fractions [Gy]						BED	EQD8
number of fractions *n*	1	2	3	4	5	15		
GTV prescription	27.02	35.83	41.79	46.33	50	68.61	100	55.56
PTV prescription	22.29	29.24	33.84	37.27	40	53.16	72	40
Bowel/Stomach constraint	15.43	20.82	24.59	27.55	30	43.48	75	25
Chest wall constraint	20	27.24	32.42	36.54	40	60	120	40

Table 1: Isoeffective/Isotoxic fractionation schemes corresponding to a tumor α/β-ratio of 10 and an α/β-ratio of 4 in all normal tissues.

		reference	spatiotemporal plan 2		spatiotemporal plan 1	
Patient	Structure	mean dose [Gy]	dose red. [%]	BED red. [%]	dose red. [%]	BED red. [%]
1 (391 cc)	GTV	51.8	9.3	0	9.5	0
5x1 fx	Liver-GTV	18.3	18.2	12.8	14.2	8.4
	Liver-PTV	16.2	19.9	17.3	15.0	11.7
2 (201 cc)	GTV	51.2	9.2	0	9.2	0
5x1 fx	Liver-GTV	11.8	16.1	8.5	11.9	4.5
	Liver-PTV	9.0	18.2	15.8	12.5	9.9
3 (207 cc)	GTV	51.6	5.8	0	5.8	0
5x1 fx	Liver-GTV	18.1	12.0	6.5	9.4	3.8
	Liver-PTV	13.0	14.7	12.7	10.7	8.5
4 (228 cc)	GTV	52.2	1.4	0	0.6	0
5x1 fx	Liver-GTV	9.0	13.7	13.0	2.0	1.4
	Liver-PTV	6.5	18.8	20.3	2.5	2.3
5 (647 cc)	GTV	51.8	8.4	0	8.2	0
5x1 fx	Liver-GTV	18.0	18.9	11.7	12.3	4.5
	Liver-PTV	10.5	29.9	28.6	16.3	13.9
1 (391 cc)	GTV	71.3	7.0	0	5.9	0
5x3 fx	Liver-GTV	23.9	12.9	8.1	9.2	4.7
	Liver-PTV	21.0	14.2	11.1	9.9	6.7
1 (391 cc)	GTV	79.8	5.4	0	5.0	0
5x5 fx	Liver-GTV	26.1	10.4	6.2	7.8	3.8
	Liver-PTV	22.8	11.5	8.5	8.4	5.4
3 (391 cc)	GTV	51.6	5.5	0	5.4	0
4+1 fx	Liver-GTV	18.1	4.0	2.4	2.5	0.7
	Liver-PTV	13.0	5.0	4.7	2.7	2.1

Table 2: Summary of liver BED reductions achieved by spatiotemporal fractionation. By definition, percentage reductions in BED and EQD8 are equal. The first column indicates patient number, total GTV volume, and treatment scheme (e.g. 5x3 fx indicates a 15-fraction treatment consisting of 5 distinct fractions delivered 3 times each).

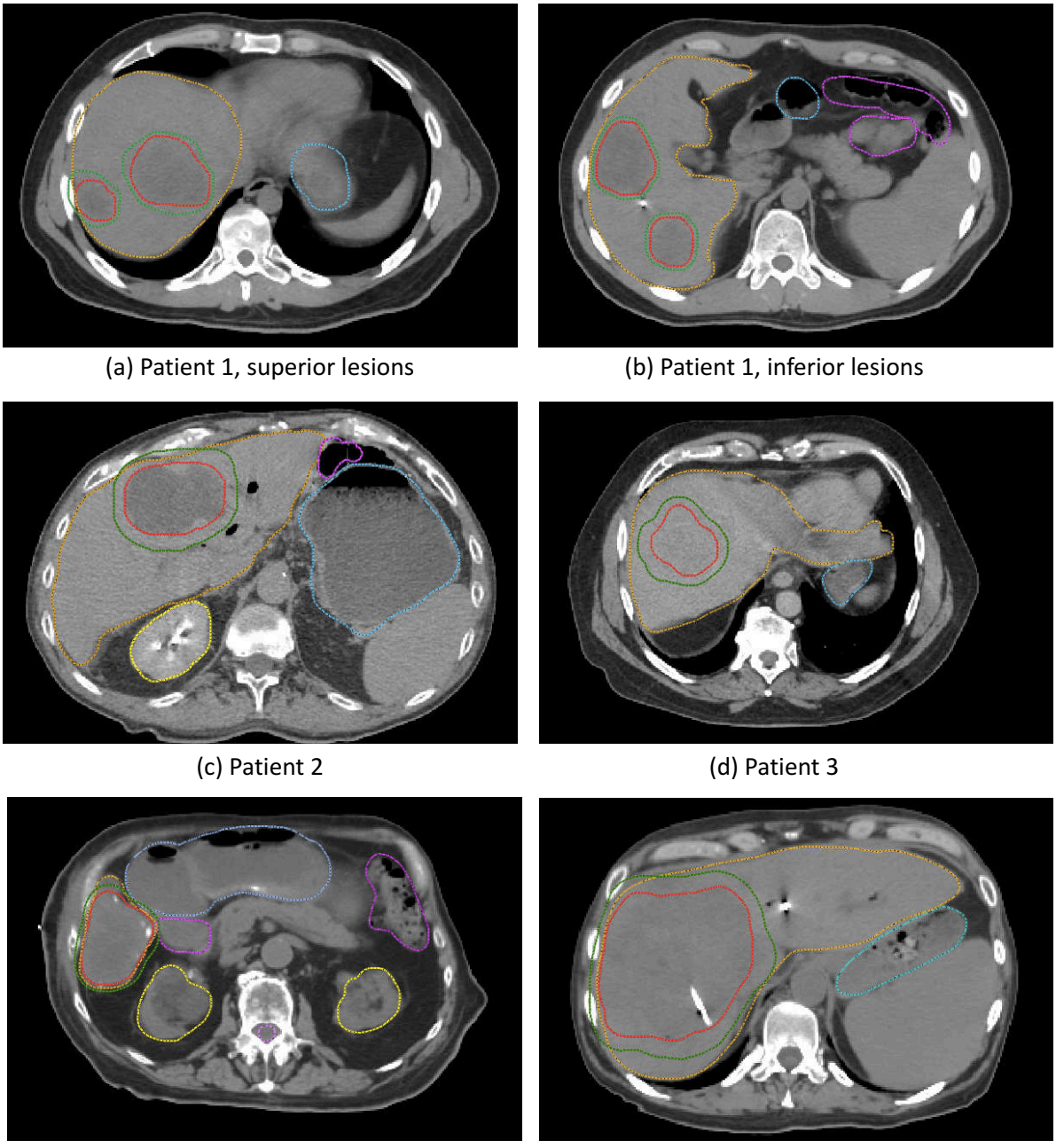

(a) Patient 1, superior lesions

(b) Patient 1, inferior lesions

(c) Patient 2

(d) Patient 3

(e) Patient 4

(f) Patient 5

Figure 1: Patient geometries. Contours show the GTV (red), PTV (green), liver (beige), stomach (blue), small and large bowel (purple), kidneys (yellow).

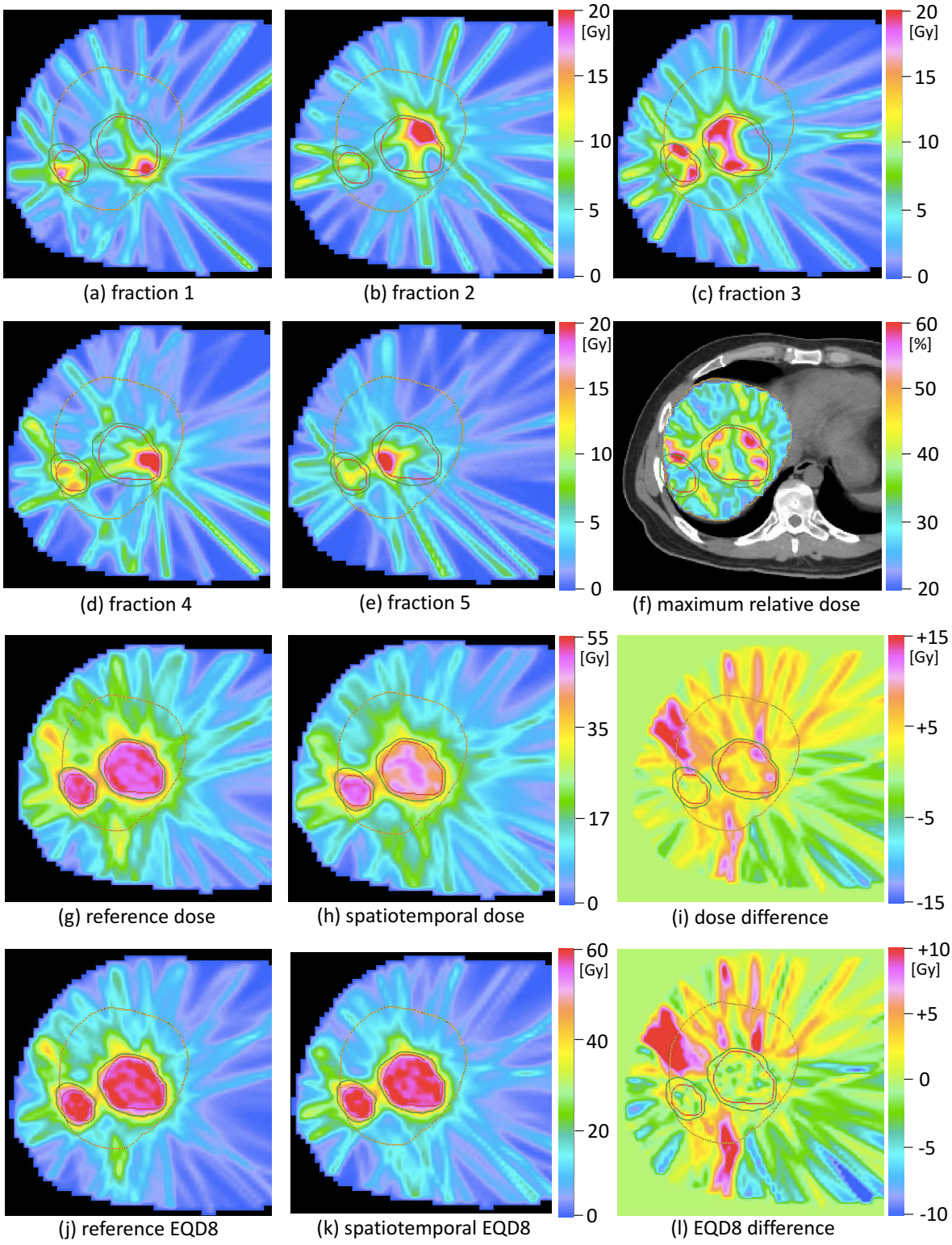

Figure 2: Comparison of reference and spatiotemporal plan 2 for the superior lesions of patient 1. (a-e) Dose distributions delivered in fractions 1-5; (f) portion of the total dose delivered by the hottest fraction; (g) physical dose of the reference plan; (h) physical dose of the spatiotemporal plan; (i) physical dose difference; (j) EQD8 for the reference plan; (k) EQD8 for the spatiotemporal plan; (l) difference in EQD8. In (i) and (l), the spatiotemporal plan is subtracted for the reference plan; positive values indicate lower doses in the spatiotemporal plan.

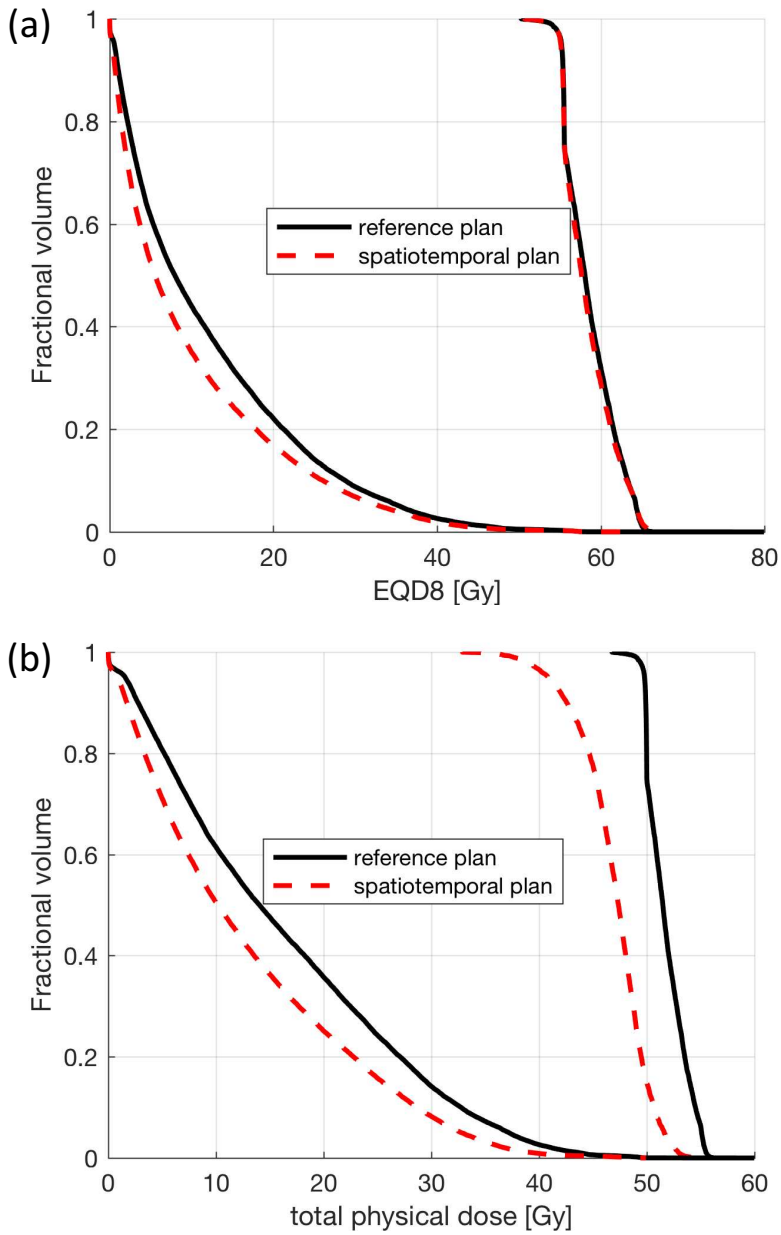

Figure 3: DVH comparison of reference plan and spatiotemporal plan 2 for patient 1 for the GTV and the liver without PTV. (a) EQD8; (b) physical dose.

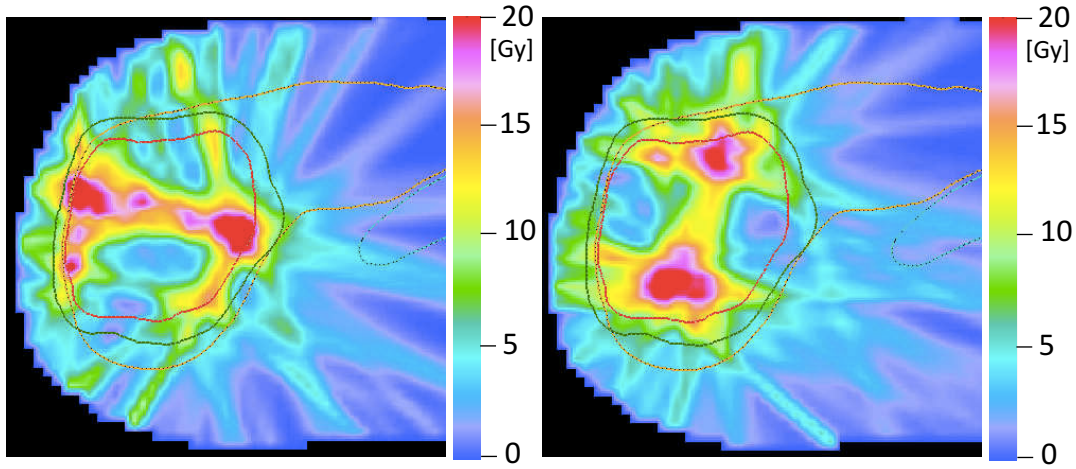

(a) patient 5

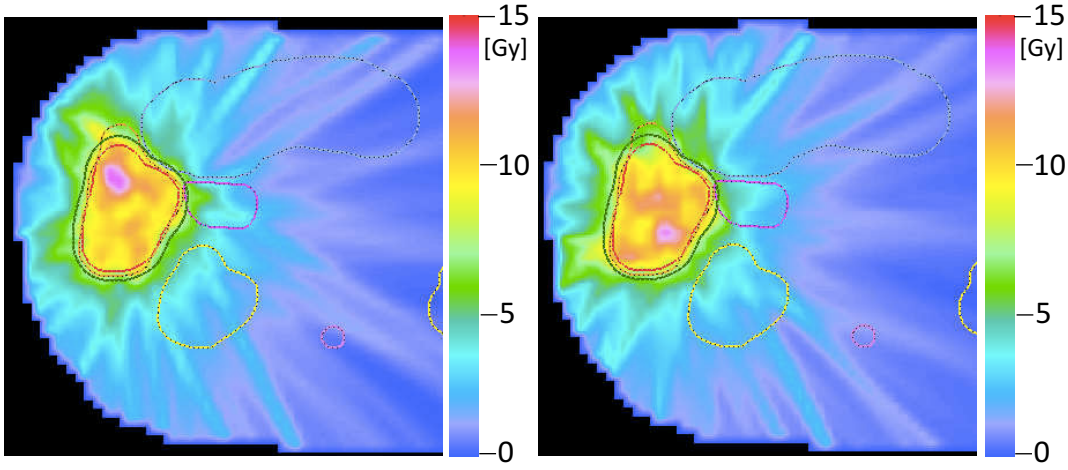

(b) patient 4

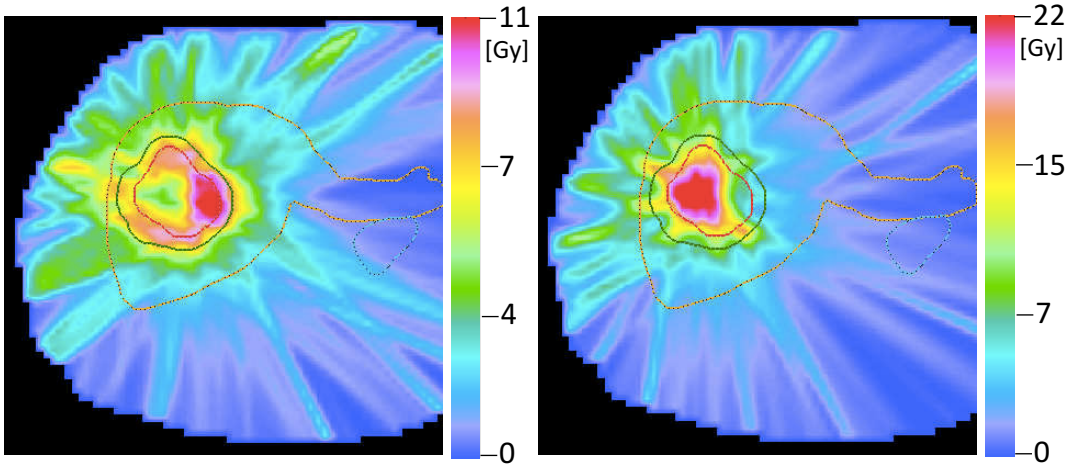

(c) patient 3, 4 + 1 fractions

Figure 4: (a,b) Two out of 5 fractions for spatiotemporal plan 2 for patient 5 (a) and patient 4 (b) in whom the tumor abuts bowel, stomach and chest wall; (c) spatiotemporal plan for patient 3 consisting of two distinct dose distributions, in which the left distribution is delivered 4 times, the right distribution once.

References:

1. Andratschke, N., et al., *Clinical results of mean GTV dose optimized robotic guided SBRT for liver metastases.* Radiat Oncol, 2016. **11**: p. 74.
2. Andratschke, N.H., et al., *Stereotactic radiation therapy for liver metastases: factors affecting local control and survival.* Radiat Oncol, 2015. **10**: p. 69.
3. Keane, F.K., et al., *Liver-Directed Radiotherapy for Hepatocellular Carcinoma.* Liver Cancer, 2016. **5**(3): p. 198-209.
4. Klement, R.J., et al., *Stereotactic body radiotherapy for oligo-metastatic liver disease - Influence of pre-treatment chemotherapy and histology on local tumor control.* Radiother Oncol, 2017.
5. Lo, S.S., et al., *Stereotactic body radiation therapy for hepatocellular carcinoma.* Discov Med, 2010. **9**(48): p. 404-10.
6. Lock, M.I., et al., *An international survey on liver metastases radiotherapy.* Acta Oncol, 2012. **51**(5): p. 568-74.
7. Velec, M., et al., *Dose escalated liver stereotactic body radiation therapy at the mean respiratory position.* Int J Radiat Oncol Biol Phys, 2014. **89**(5): p. 1121-8.
8. Chang, D.T., et al., *Stereotactic body radiotherapy for colorectal liver metastases: a pooled analysis.* Cancer, 2011. **117**(17): p. 4060-9.
9. Rusthoven, K.E., et al., *Multi-institutional phase I/II trial of stereotactic body radiation therapy for liver metastases.* J Clin Oncol, 2009. **27**(10): p. 1572-8.
10. Hall, E.J. and A.J. Giaccia, *Radiobiology for the radiologist*. 7th ed. 2012, Philadelphia, Pa.: Lippincott Williams & Wilkins. 546 S.
11. Unkelbach, J. *Non-uniform spatiotemporal fractionation schemes in photon radiotherapy*. in *World Congress on Medical Physics and Biomedical Engineering, June 7-12, 2015, Toronto, Canada*. 2015. Springer.
12. Unkelbach, J., et al., *Spatiotemporal Fractionation Schemes for Irradiating Large Cerebral Arteriovenous Malformations.* Int J Radiat Oncol Biol Phys, 2016. **95**(3): p. 1067-74.
13. Unkelbach, J. and D. Papp, *The emergence of nonuniform spatiotemporal fractionation schemes within the standard BED model.* Med Phys, 2015. **42**(5): p. 2234-41.
14. Unkelbach, J., C. Zeng, and M. Engelsman, *Simultaneous optimization of dose distributions and fractionation schemes in particle radiotherapy.* Med Phys, 2013. **40**(9): p. 091702.
15. Fowler, J.F., *21 years of biologically effective dose.* Br J Radiol, 2010. **83**(991): p. 554-68.
16. Bentzen, S.M., et al., *Bioeffect modeling and equieffective dose concepts in radiation oncology--terminology, quantities and units.* Radiother Oncol, 2012. **105**(2): p. 266-8.
17. Unkelbach, J., et al., *Optimization approaches to volumetric modulated arc therapy planning.* Med Phys, 2015. **42**(3): p. 1367-77.
18. Pan, C.C., et al., *Radiation-associated liver injury.* Int J Radiat Oncol Biol Phys, 2010. **76**(3 Suppl): p. S94-100.
19. Bangert, M., P. Hennig, and U. Oelfke, *Analytical probabilistic modeling for radiation therapy treatment planning.* Phys Med Biol, 2013. **58**(16): p. 5401-19.
20. Unkelbach, J. and U. Oelfke, *Inclusion of organ movements in IMRT treatment planning via inverse planning based on probability distributions.* Phys Med Biol, 2004. **49**(17): p. 4005-29.

21. Witte, M.G., et al., *IMRT optimization including random and systematic geometric errors based on the expectation of TCP and NTCP.* Med Phys, 2007. **34**(9): p. 3544-55.
22. Dempsey, J., et al., *A device for realtime 3D image-guided IMRT.* International Journal of Radiation Oncology• Biology• Physics, 2005. **63**: p. S202.
23. Lagendijk, J.J., B.W. Raaymakers, and M. van Vulpen. *The magnetic resonance imaging–linac system*. in *Seminars in radiation oncology*. 2014. Elsevier.
24. Raaymakers, B.W., et al., *Integrating a 1.5 T MRI scanner with a 6 MV accelerator: proof of concept.* Phys Med Biol, 2009. **54**(12): p. N229-37.
25. Booth, J.T., et al., *The first patient treatment of electromagnetic-guided real time adaptive radiotherapy using MLC tracking for lung SABR.* Radiother Oncol, 2016. **121**(1): p. 19-25.
26. Brix, L., et al., *Three-dimensional liver motion tracking using real-time two-dimensional MRI.* Med Phys, 2014. **41**(4): p. 042302.
27. Colvill, E., et al., *A dosimetric comparison of real-time adaptive and non-adaptive radiotherapy: A multi-institutional study encompassing robotic, gimbaled, multileaf collimator and couch tracking.* Radiother Oncol, 2016. **119**(1): p. 159-65.
28. Crijns, S.P., B.W. Raaymakers, and J.J. Lagendijk, *Proof of concept of MRI-guided tracked radiation delivery: tracking one-dimensional motion.* Phys Med Biol, 2012. **57**(23): p. 7863-72.
29. Ehrbar, S., et al., *Respiratory motion-management in stereotactic body radiation therapy for lung cancer - A dosimetric comparison in an anthropomorphic lung phantom (LuCa).* Radiother Oncol, 2016. **121**(2): p. 328-334.
30. Keall, P.J., et al., *The first clinical implementation of electromagnetic transponder-guided MLC tracking.* Med Phys, 2014. **41**(2): p. 020702.
31. Nguyen, D.T., et al., *The first clinical implementation of a real-time six degree of freedom target tracking system during radiation therapy based on Kilovoltage Intrafraction Monitoring (KIM).* Radiother Oncol, 2017. **123**(1): p. 37-42.
32. Ehrbar, S., et al., *Validation of Dynamic Treatment-Couch Tracking for Prostate SBRT.* Med Phys, 2017.

Supplementary material

for the paper

Spatiotemporal fractionation schemes for liver stereotactic body radiotherapy

A Patients

Five patients were selected as to represent a spectrum of tumor geometries, locations and sizes. Patient 1 has 4 metastases of varying size located throughout the right lobe of the liver and the total GTV volume is 391 cc. Patient 2 has one lesion (201 cc) peripherally located in the right lobe; patient 3 has one large and one small metastasis centrally located in the right lobe with a total GTV volume of 207 cc; patient 4 has a single lesion in the inferior part of the right lobe (228 cc), which abuts the small bowel, the stomach, and chest wall; patient 5 has one very large lesion (647 cc) in the inferior part of the liver.

B Treatment plan optimization

In this section we detail the treatment plan optimization methods. Simultaneous optimization for multiple treatment plans for spatiotemporal fractionstion is based on objective and constraint functions evaluated for cumulative BED b.

B.1 Optimization of reference plan and spatiotemporal plan 1

We solve the following optimization problem:

$$\begin{aligned}
\text{minimize} \quad f(\boldsymbol{b}) &= \frac{1}{N_G}\sum_{i\in G}\left[10\,(100-b_i)_+^2+(b_i-115.5)_+^2\right] \quad (\text{GTV},\ \alpha/\beta=10) && (1)\\
&+ \frac{1}{N_P}\sum_{i\in P}\left[10\,(72-b_i)_+^2+(b_i-100)_+^2\right] \quad (\text{PTV},\ \alpha/\beta=10) && (2)\\
&+ \frac{10}{N_W}\sum_{i\in W}(b_i-120)_+^2 \quad (\text{Chest wall overdose},\ \alpha/\beta=4) && (3)\\
&+ \frac{1}{N_R}\sum_{i\in R}\left(b_i-b_i^{\max}\right)_+^2 \quad (\text{conformity},\ \alpha/\beta=4) && (4)\\
&+ \frac{1}{N_H}\sum_{i\in H}b_i \quad (\text{mean BED remaining healthy tissues},\ \alpha/\beta=4) && (5)\\
&+ \frac{1}{N_L}\sum_{i\in L}b_i \quad (\text{mean BED in the liver without GTV},\ \alpha/\beta=4) && (6)\\
\\
\text{subject to} \quad b_i &\le 75 \quad \forall i\in O \quad (\text{maximum BED in OARs},\ \alpha/\beta=4) && (7)\\
b_i &= \sum_{t=1}^{T} n_t\left(d_{ti}+\frac{(d_{ti})^2}{(\alpha/\beta)_i}\right) \quad \forall i \quad (\text{BED in voxel } i \text{ in fraction } t) && (8)\\
d_{ti} &= \sum_j D_{ij}x_{tj} \quad \forall i,t \quad (\text{physical dose in voxel } i \text{ in fraction } t) && (9)\\
x_{tj} &\ge 0 \quad \forall j,t \quad (\text{non-negative fluence}) && (10)
\end{aligned}$$

Here, t indexes the fractions that deliver distinct dose distributions, T is the number of distinct dose distributions, and n_t is the number of times fraction t is delivered. Hence, for the reference plan we have $T=1$. x_{tj} denotes the fluence of beamlet j in fraction t and d_{ti} are the physical doses per fraction in voxel i in fraction t. The dose-deposition matrix elements D_{ij} denotes the dose contributions of beamlets j to voxel i for unit fluence. G and P denote the sets of voxels contained in the GTV and the PTV, respectively; W is the set of voxels in the chest wall; L denotes all voxels in the liver excluding the GTV; R is the set of voxels in a 1 cm margin of normal tissue surrounding the PTV; O denotes the union of voxels in the duodenum, small bowel, large bowel, and stomach; and H is the set of all normal tissue voxels outside of the PTV that are not in L.

The maximum BED $b_i^{\max}$ in the conformity objective depends linearly on the euclidean distance z_i of a normal tissue voxel i from the PTV contour:

$$b_i^{\max} = 175 - z_i\,(175-40) \tag{11}$$

Hence, a falloff of the BED from 175 Gy at the edge of the PTV to 40 Gy at 1 cm distance is aimed for, corresponding to a physical dose fall-off from 50 Gy to 20 Gy for a uniformly

fractionated 5-fraction treatment.

To find a local minimum of the optimization problem, we use our own implementation of the L-BFGS quasi-Newton method [3], together with an augmented Lagrangian method for handling constraints [1]. Calculation of the dose-deposition matrix elements D_{ij} is performed with the open-source radiotherapy planning research platform CERR [2]. Fluence maps were initialized with small random intensities.

B.2 Optimization of spatiotemporal plan 2

We denote the objective values for the GTV, PTV, chest wall, conformity, and healthy tissue obtained in the reference plan by f_G^{ref}, f_P^{ref}, f_W^{ref}, f_R^{ref}, and f_H^{ref}. To obtain the spatiotemporal plan 2, we solve the following optimization problem:

$$\text{minimize} \quad \frac{1}{N_L}\sum_{i\in L} b_i \quad \text{(mean liver BED)} \tag{12}$$

$$\begin{aligned}
\text{subject to} \quad f_G^{\text{ref}} &\geq \frac{1}{N_G}\sum_{i\in G}\left[10\left(100-b_i\right)_+^2+\left(b_i-115.5\right)_+^2\right] && (13)\\
f_P^{\text{ref}} &\geq \frac{1}{N_P}\sum_{i\in G}\left[10\left(72-b_i\right)_+^2+\left(b_i-100\right)_+^2\right] && (14)\\
f_W^{\text{ref}} &\geq \frac{10}{N_W}\sum_{i\in W}\left(b_i-120\right)_+^2 && (15)\\
f_R^{\text{ref}} &\geq \frac{1}{N_R}\sum_{i\in R}\left(b_i-b_i^{\max}\right)_+^2 && (16)\\
f_H^{\text{ref}} &\geq \frac{1}{N_H}\sum_{i\in H} b_i && (17)\\
b_i &\leq 75 \quad \forall i\in O && (18)\\
b_i &= \sum_{t=1}^{T} n_t\left(d_{ti}+\frac{(d_{ti})^2}{(\alpha/\beta)_i}\right) \quad \forall i && (19)\\
d_{ti} &= \sum_j D_{ij}x_{tj} \quad \forall i,t && (20)\\
x_{tj} &\geq 0 \quad \forall j,t && (21)
\end{aligned}$$

To obtain the spatiotemporal plan 2, the same optimization algorithm was used. The fluence maps were initialized using the spatiotemporal plan 1 with small random perturbations. Spatiotemporal plans 1 and 2 therefore resulted in qualitatively similar solutions.

C Results

C.1 Spatiotemporal treatment plans

Figure 5 shows the fractional doses delivered in the spatiotemporal treatment plans 2 for all patients. The treatment plans for patients 1, 2, 3 and 5 have in common that each fraction delivers high single fraction doses to complementary parts of the tumor. This compartmentalization of the target volume is not manually determined. Instead, these dose distributions are found automatically through the optimization algorithm. The results for large tumors, such as for patient 5, show that the best treatment plans to achieve partial hypofractionation in the tumor along with more uniform fractionation in the normal liver are not obvious. Such plans would be difficult to design manually. Patient 4 differs from the remaining patients as the tumor is surrounded by OARs with maximum BED constraint. Therefore, only a small degree of hypofractionation is achieved in the tumor as described in the main manuscript. The spatiotemporal plans 1 show the same qualitative features and similar dose distributions as the spatiotemporal plans 2.

C.2 Quantifying the benefit of spatiotemporal fractionation

In this paper, we report two spatiotemporal treatment plans to quantify the benefit over the uniformly fractionated reference plan. Spatiotemporal plan 1 is obtained by minimizing the same objective function as for the reference plan. Thereby, the benefit of spatiotemporal fractionation is distributed over multiple objectives. The spatiotemporal plan 1 reduces mean liver BED but also improves on target coverage and conformity. This has the disadvantage that the improvement is difficult to quantify. In spatiotemporal plan 2, the mean liver BED is minimized as the only objective, subject to the constraints that the plan is no worse than the reference plan in any other objective. Thereby all benefit of spatiotemporal fractionation is shifted into reduction of mean liver BED. This has the advantage that the improvement of the reference plan can quantified by a single number. However, it can lead to misleading observations in certain situations as seen for patients 4 and 5.

For patient 4, a large discrepancy between spatiotemporal plan 1 and 2 regarding their liver BED reduction is observed (Table 2). For spatiotemporal plan 1, a small mean liver BED of 2% is observed. This is expected because the dose distributions delivered in each of the 5 fractions is similar. The mean physical dose in the GTV is only 1% lower than in the reference plan. This is due to the maximum BED constraint for OARs surrounding the tumor, which are best protected through uniform fractionation. For spatiotemporal plan 2, a large improvement is observed, which is not explained by the effects of spatiotemporal fractionation alone. It is rather due to the location of spatiotemporal plan 1 on the pareto surface that characterizes the tradeoff between the 6 objectives. For this patient, a small relaxation of the first 5 objectives happens to allow for a large improvement in mean liver BED, the 6th objective. Hence, the large benefit observed for spatiotemporal plan 2 is technically correct but misleading.

A similar effect is observed for patient 5. The large benefit of 29% in spatiotemporal plan 2 is

not explained by the effects of spatiotemporal fractionation alone. For this patient the tumor involves most of the right lobe. The degree to which the left lobe can be spared depends on the conformity of the plan and the dose delivered to the remaining healthy tissue outside of the liver. By sacrificing conformity, the dose delivered to the left lobe of the liver can be reduced substantially. Spatiotemporal plan 1 yields improvements to all 6 objectives relative to the reference plan. Compared to spatiotemporal plan 1, the first 5 objectives are relaxed in spatiotemporal plan 2, which allows for an overproportionate improvement in the mean liver BED.

References

[1] DP Bertsekas. *Nonlinear programming.* Athena Scientific, 1999.

[2] J.O. Deasy, A.I. Blanco, and V.H. Clark. CERR: a computational environment for radiotherapy research. *Medical physics*, 30:979, 2003.

[3] SJ Wright and J Nocedal. *Numerical optimization*, volume 2. Springer New York, 1999.

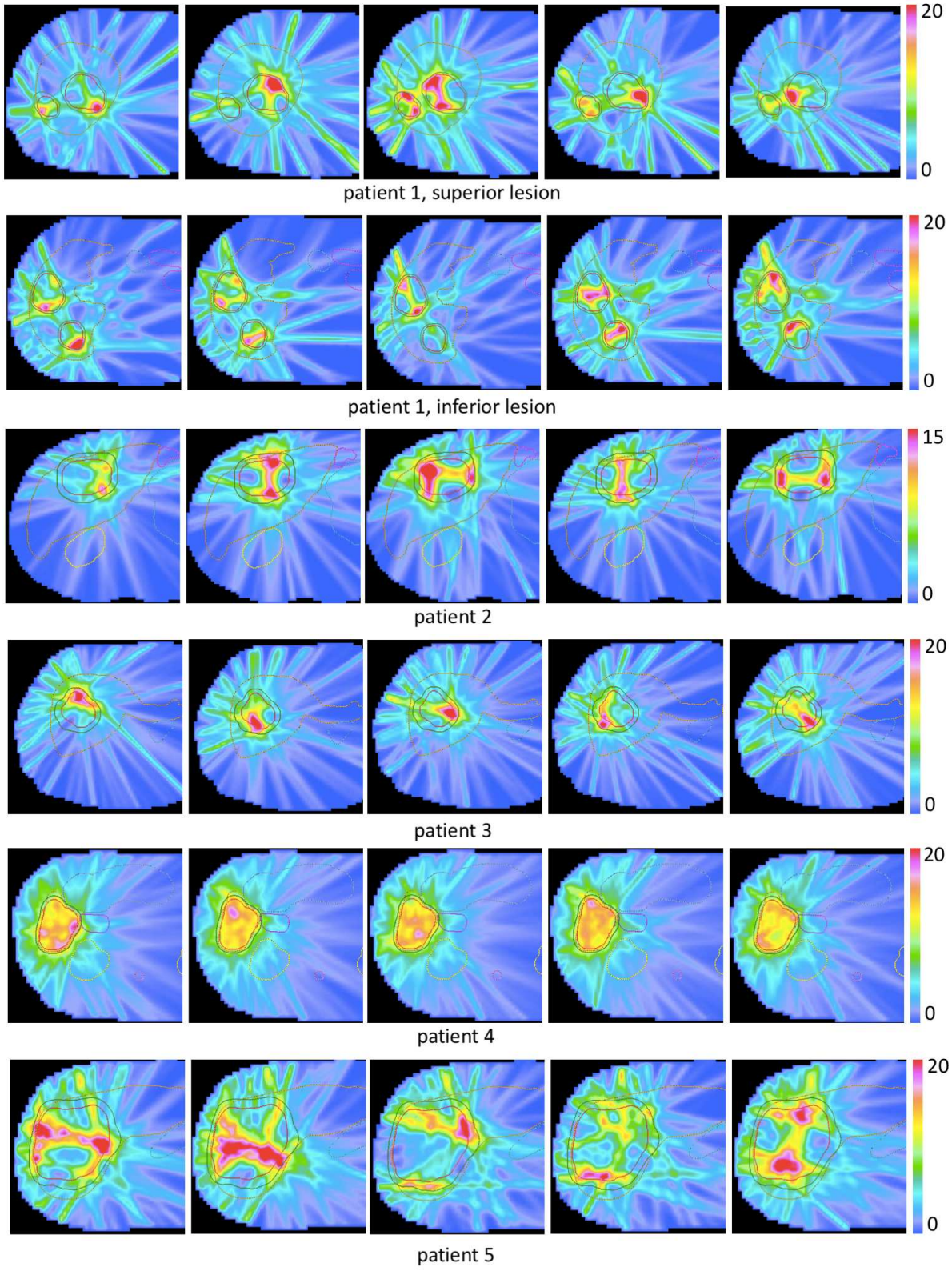

Figure 5: Dose distributions delivered in 5 fractions for spatiotemporal plan 2.